EUROPEAN ORGANIZATION FOR NUCLEAR RESEARCH

CERN/EP 81-12
18 January 1981

PRODUCTION OF VECTOR AND TENSOR MESONS IN PROTON-PROTON COLLISIONS AT $\sqrt{s}$ = 52.5 GeV

Annecy-CERN-Collège de France-Dortmund-Heidelberg-Warsaw Collaboration

D. Drijard, H.G. Fischer, W. Geist, P.G. Innocenti, V. Korbel*, A. Minten
A. Norton, S. Stein**, O. Ullaland and H.D. Wahl***
CERN, European Organization for Nuclear Research, Geneva, Switzerland

G. Fontaine, C. Ghesquière and G. Sajot
Collège de France, Paris, France

P. Hanke+, W. Hofmann, M. Panter, K. Rauschnabel, J. Spengler and
D. Wegener
Institut für Physik der Universität Dortmund, Germany

H. Frehse+, M. Heiden, E.E. Kluge and A. Putzer
Institut für Hochenergiephysik der Universität Heidelberg, Germany

M. Della Negra and D. Linglin
LAPP, Annecy, France

R. Gokieli and R. Sosnowski
Institute for Nuclear Research, Warsaw, Poland

Submitted to Zeitschrift für Physik C

---

* Now at DESY, Hamburg
** Now at BNL, Brookhaven, USA
*** Now at Institut für Hochenergiephysik, Österr. Akademie der Wissenschaften, Wien, Austria
\+ Now at CERN, Geneva, Switzerland

EP/0402P/PH/ef

ABSTRACT

Inclusive production of ρ^0, f and g^0 mesons and of K^0_S, $K^{*0}(892)$, ϕ and $K^{*0}(1430)$ mesons has been measured at $\langle y \rangle \sim 2.6$ and $\langle p_T \rangle \sim 1.1$ GeV/c in proton-proton interactions at $\sqrt{s}$ = 52.5 GeV. The negative particle from the two-body decays of these resonances were identified by a threshold Cerenkov counter and used for triggering. Starting from the measured differential cross section, total inclusive cross sections for the vector and tensor mesons were determined using various parametrizations for the y and p_T dependence of the differential cross section. The experimental results are discussed in the framework of production models based on the parton picture. The strangeness suppression factor $\lambda = (0.30 \pm 0.10)$ due to SU(3) symmetry breaking of the quark sea is derived.

1. INTRODUCTION

The investigation of vector and tensor meson production in hadronic interactions is important for the explanation [1] of short range correlations, which represent a major dynamical feature of inelastic hadronic interactions [2]. Moreover, vector meson production is of high significance for the interpretation of hadronic production processes in the framework of the quark parton model [3]. Especially the production of mesons in the region of large Feynman x is of great interest, since recently a connection between the particle spectra in this kinematical region and the structure functions of hadrons, as observed in deep inelastic processes, has been established [4]. Moreover, the comparison of the production cross section of vector and tensor mesons with different strangeness allows to study the SU(3) symmetry breaking of the quark sea and the influence of angular momenta $L > 0$ on the quark fragmentation process.

The investigation of ϕ meson production might reveal special features, since it is the lightest vector meson built solely from sea quarks of the proton. It shares this property with the heavier vector mesons with hidden new flavours like e.g. ψ, T. Models which claim to describe the production of hidden new flavours may therefore also be applicable to the production of ϕ mesons.

The present paper describes the results of an experiment, in which forward production of vector and tensor mesons with and without strangeness has been measured at a center of mass energy of $\sqrt{s} = 52.5$ GeV. The paper is organized as follows. The apparatus and data reduction are described in sect. 2. In sect. 3 the method of extracting the resonance signal is discussed. The resulting cross sections are compiled in sect. 4; they are compared to results of previous experiments and model predictions in sect. 5. In sect. 6 the conclusions are summarized. A detailed description of the presented data is given in ref. [5].

2. EXPERIMENT AND DATA REDUCTION

The experiment was performed at the CERN Intersecting Storage Rings (ISR) using the Split Field Magnet Detector (SFM). The details of the

experimental set-up, the trigger, the data acquisition, reduction and analysis have been described in previous publications [6,7]. The results discussed in this paper are based on data samples obtained by triggering on a negative particle in the kinematical interval $0.2 < x < 0.6$ ($\langle x \rangle = 0.31$) and 0.5 GeV/c $< p_T < 2$ GeV/c ($\langle p_T \rangle = 1.15$ GeV/c).

A threshold Cerenkov counter, covering the trigger region, allowed the separation of a "pion" and a "non-pion" sample [8]. Each of the samples consisted of approximately 100 000 events. The threshold Cerenkov counter had an efficiency larger than 99.6 %. The π^- meson sample has a contamination of less than 1% due to other particles, while in the "non-pion" sample $\sim$ 80% of the trigger particles are K^- mesons, 20% are antiprotons [9] and the contamination of pions is smaller than 2%. In the present analysis the trigger particle in the "non-pion" sample has been assumed to have the mass of a K^- meson. In the "non-pion" sample the production of D^+ mesons [10] and the charmed baryon Λ_c^+ [11] has been observed.

3. DETERMINATION OF RESONANCE SIGNALS

3.1 $\pi^-\pi^+$ invariant mass spectrum

The data sample with an identified π meson as a trigger particle was used to determine the invariant mass spectrum of $\pi^-\pi^+$ systems. All positive particles were treated as pions. This mass assumption is a good approximation for $|x_+| < 0.4$ [9], which corresponds to the phase space region populated dominantly by decay products of the resonances under investigation in the present experiment.

Fig. 1(a) shows the measured $\pi^-\pi^+$ mass spectrum. Above a strong background from non-resonant $\pi^-\pi^+$ pairs (solid line) two peaks are observed in the mass interval of the ρ^0 meson and the f meson. Due to the different Q values, the strength of the resonance signals as well as the shape of the non-resonant background depend on the relative position of the π^- meson and of the π^+ meson in phase space. To study this effect, which turns out to provide a cross check for background calculations, in figs 1(b) and 1(c) the mass spectra are plotted for $\pi^-\pi^+$ pairs in the azimuthal angular region ($|\phi(\pi^-)-\phi(\pi^+)| < 90°$, π^+ closed pairs) and the opposite azimuthal angular

region ($|\phi(\pi^-)-\phi(\pi^+)| > 90°$, π^+ open pairs) respectively. In fig. 1(b) the dominating resonance signal is due to the ρ^0 meson, in addition a weaker signal from the f meson is observed. If the π^+ meson is detected opposite in azimuth to the π^- meson trigger (fig. 1(c)), the dominant resonance signal stems from the f meson; in addition weaker contributions from the ρ^0 meson and the g^0 meson show up. For all three cases the non-resonant background of $\pi^-\pi^+$ pairs (solid lines) peaks in the region of the dominant resonant signal.

To determine the shape of the background due to non-resonant $\pi^-\pi^+$ pairs, the positive pions from one event were combined with the triggering π^- meson from other events ("mixed events"). The background of uncorrelated $\pi^-\pi^+$ pairs constructed in this way is expected to take into account automatically the inefficiencies of the detector and of the pattern recognition program as well as phase space effects. Since the trigger tracks in the event sample of the present experiment are confined to a small region of the phase space, energy momentum conservation is not expected to be strongly violated for the sample of "mixed events". Higgens et al., [12] have pointed out the importance of this constraint for a proper background reconstruction. The uncorrelated background signal, generated in the described way, has been included into figs 1(a-c). Generally it describes the $\pi^-\pi^+$ mass spectrum properly outside the resonance region.

To extract the resonance signal, the uncorrelated background plus resonance contributions from ρ^0 meson, f meson and g^0 meson have been fitted to the measured invariant mass distribution in the mass interval $0.3\ \text{GeV} < m_{\pi\pi}c^2 < 4\ \text{GeV}$ by minimization of χ^2. The resonance signals have been parametrized by a relativistic Breit-Wigner formula with mass dependent width [13]:

$$\sigma_{BW}(m) \sim \frac{m\, m_0\, \Gamma(m)}{(m_0^2-m^2)^2 + (m_0\Gamma(m))^2} \tag{1}$$

$$\Gamma(m) = \Gamma_0 \left(\frac{q}{q_0}\right)^{2L+1} \frac{2q_0^2}{q^2 + q^2{}_0} \tag{2}$$

The parameters have the following meaning: m_0, Γ_0 are the resonance mass and width respectively; L is the relative angular momentum of the

decay products; q and q_0 are the momenta of the decay products in the rest frame of the resonance for the invariant masses m and m_0 respectively.

In the fit the resonance mass m_0 and the width Γ_0 were treated as free parameters. The number of events in the resonance peak was determined separately for the figs 1(a), (b) and (c). Within statistical error the number of events in the resonance peak of fig. 1(a) agrees with the corresponding sum of event numbers obtained from figs 1(b) and (c). The observed shift of the resonance masses m_0 in the present analysis, compared to the standard values [14], is compatible with known local systematic errors of the SFM detector [5,10]. The fitted value of the resonance width Γ_0 agrees with the value calculated from the natural width of the resonance [14] folded with resolution of the SFM in the mass region investigated.

In figs 2(a-c) the invariant mass spectra corresponding to figs 1(a-c) are plotted after the subtraction of the uncorrelated $\pi^-\pi^+$ pair background. Peaks due to the K_s^o meson, ρ^0 meson, f meson and g^0 meson show up clearly. The influence of the phase space cuts (azimuthal angle) on the strength of the resonance signals are obvious. In fig 2(c) the contribution from ρ^0 and f meson decays (full line) to the invariant mass spectrum is smaller than the observed number of combinations in the interval around $m_{\pi\pi} \sim 1$ GeV/c². This additional contribution can be explained as a reflection of the $A_2^{o,+}$ meson three-body decay, if one assumes in accordance with the SU(3) quark model prediction [15] that the A_2 meson production cross section is as large as that of the f meson [5].

In table 1 the results from the analysis of the $\pi^-\pi^+$ invariant mass distribution are collected. The number of events as observed in the resonance peak N_R in our experiment is taken as the mean value

$$N_R = \frac{1}{2}\,(N_a + N_b + N_c)\ , \qquad (3)$$

where N_i (i = a,b,c) corresponds to the signal as derived from figs 1(a-c) respectively. Within the error limits the relation $N_a = N_b + N_c$ holds. This result provides a consistency check of the background determination. The significance of all resonance signals is higher than 6 s.d.

3.2 $K^-\pi^+$ invariant mass spectrum

The data sample with a triggering negative particle, which produced no Cerenkov signal, has been analyzed in a similar manner as described in sect. 3.1 for the π meson sample. In the "non-pion" data set the K^- meson mass was assigned to all trigger particles, while again all positive particles were treated as pions. The measured $K^-\pi^+$ invariant mass spectrum of the full data sample is given in fig. 3. The non-resonant background of $K^-\pi^+$ pairs, determined in the same way as described in sect. 3.1 for $\pi^-\pi^+$ pairs from different events, is included as solid line in fig. 3. Clear resonance signals appear in the $\overline{K^{*0}}(892)$ and the $\overline{K^{*0}}(1430)$ resonance. In addition, a structure is observed in the mass interval around 1.2 GeV/c^2. This enhancement is due to a reflection [5] of the three-body decay

$$\overline{K^{*0}}(1430) \rightarrow K^{*-}(892)\ \pi^+ \rightarrow K^-\pi^0\pi^+ \ . \qquad (4)$$

It has been checked [5] that the observed $\overline{K^{*0}}(892)$ peak is not due to a reflection from $\overline{\Delta^0} \rightarrow \bar{p}\pi^+$ decay.

Subtracting the uncorrelated background from the measured $K^-\pi^+$ invariant mass spectrum, the distribution shown in fig. 4 is obtained. The small peak observed in fig. 4 in the threshold region is a reflection of the $\bar{\Lambda} \rightarrow \bar{p}\pi^+$ decay, where the antiproton was wrongly assigned the K^- meson mass in the present analysis. The cross checks discussed in sect. 3.1 for the $\pi^-\pi^+$ mass distributions have also been performed for the $K^-\pi^+$ spectra. The results of the analysis are collected in table 2.

3.3 K^-K^+ invariant mass spectrum

Taking the K^- meson event sample and treating alternatively all positive particles as K^+ mesons, one gets the invariant mass spectrum shown in fig. 5(a). A clear ϕ meson signal is observed at the proper mass with a width compatible with the mass resolution of the detector. The background from uncorrelated K^-K^+ pairs determined again by event mixing is included in fig. 5(a) (solid line). It describes the observed mass distribution in a broad interval excluding the mass bin of the ϕ meson. One obtains fig. 5(b) after the subtraction of the background from the

measured invariant mass distribution. The number of events in the ϕ resonance signal is included in table 2. To indicate the statistical significance of the ϕ meson signal and the size of fluctuations at higher masses due to the increasing background (fig. 5(a), the dashed line corresponding to 2 s.d. fluctuations of background, is included in fig. 5(b).

Because of the small Q value for the $\phi \to K^+K^-$ decay, the observed ϕ meson signal cannot be due to a reflection of a resonance in the $K^-\pi^+$ channel. To check the consistency of the background determination, we have used the π^- meson sample to determine the background in an independent way. For this purpose we have ascribed to the trigger π^- meson the K^- meson mass and have treated all positive particles as K^+ mesons. The background, determined in this way, is in excellent agreement with the one derived by the event mixing method. This result proves the consistency of the background calculations.

4. CROSS SECTION

4.1 Corrections

The inclusive cross section for meson resonance production has been determined by Monte-Carlo methods, taking account of the experimental acceptance, the efficiency of the reconstruction program and the cuts applied to the invariant mass spectra. The experimental acceptance correction includes the efficiency of the specially designed trigger system [6,7], the acceptance of the Cerenkov counters and the efficiency for charged particle detection of the SFM detector. Generating a sample of $\pi^-(K^-)$ meson events into the same acceptance region as the resonance signal, the absolute normalization is obtained by comparison with published $\pi^-(K^-)$ meson data [9,17]. For the K^- meson trigger sample, the $\bar{p}$ admixture was corrected for.

The acceptance region Ω_R for meson resonances covers a sizeable fraction of phase space, larger than the corresponding region for the trigger particle Ω_T. Consequently, our global acceptance for resonances in Ω_R, and the resulting estimated cross section $(\sigma.B)_{\Omega_R}$, are sensitive to the

momentum dependence of resonance production. We assumed scaling and approximate factorization in the form

$$E \frac{d^3\sigma}{dp^3} \sim f(y) \frac{d\sigma}{dp_T^2} \quad . \tag{5}$$

In agreement with observations at low energies [16], we have assumed that the produced resonances are unpolarized and therefore their decay angular distribution was chosen to be isotropic. Since the p_T and the y dependences are not determined in the present experiment, which recorded only data in a limited phase space region, we have used parametrizations of the shape of the inclusive cross section as derived from other experiments.

The details are given separately for each resonance in sect. 4.2. The total uncertainty of the resonance cross sections includes the uncertainty of normalization for the π^- meson (10%) and the K^- meson cross sections (15%), the statistical uncertainty of the resonance signal given in tables 1 and 2, the uncertainty in the acceptance calculation for $\pi^-(K^-)$ mesons and the resonances ($\sim$ 20%) and the uncertainty of the branching ratios B of the resonance decay into the channel investigated. In addition for the K^- meson trigger the uncertainty of the $\bar{p}$ admixture was considered.

4.2 Resonance cross sections

In order to determine the total and differential cross section of resonance production, we have to assume the form of its p_T and y dependence. In this paper either these dependences are taken from other experiments at lower energies or are derived from scaling laws, if no other data are available. In the following only the results based on the most reasonable parametrization are discussed. A more detailed discussion of the different parametrizations and the results is given in ref. [5].

4.2.1 K_s^o meson production

The quark content of the detected K_s^o meson is comparable to the quark composition of a mixture of charged K mesons.

Since the longitudinal and transverse dependences of differential cross sections depend on the quark content of the produced particles [3], the x dependence of the invariant cross section for K_s^o meson production is expected to lie in between those for K^- and K^+ meson production [18]

$$K^+ : x \frac{d\sigma}{dx} \sim (1-x)^{3.2 \pm 0.3} , \tag{6}$$

$$K^- : x \frac{d\sigma}{dx} \sim (1-x)^{5.8 \pm 0.2} . \tag{7}$$

This expectation is in agreement with measured K_s^o meson production cross section at $\sqrt{s}$ = 27.4 GeV [19]

$$K_s^o : x \frac{d\sigma}{dx} \sim (1-x)^{5.0 \pm 0.5} . \tag{8}$$

The same p_T dependence of the K_s^o production cross section as that for charged mesons $K^{\pm}$ was assumed. In summary we used the following parametrization

$$E \frac{d^3\sigma}{dp^3} \sim (1-x)^5 e^{-5p_T} . \tag{9}$$

The resulting differential and total cross sections of the present experiment are given in table 3.

4.2.2 ρ^0 meson production

ρ^0 meson production in pp collisions has been studied extensively especially at lower energies. We have used in our analysis the parametrization of the y and p_T dependence for the ρ^0 meson production cross section of ref. [20]. The results of our experiment for the differential and the total cross sections are collected in table 3. The total cross section of the present experiment and that one of ref. [20] are in good agreement.

4.2.3 f meson production

Results of an experiment at $\sqrt{s}$ = 27.4 GeV [21] have been exploited to determine the dependence of the invariant cross section on the rapidity y and the transverse momentum p_T. The transverse momentum dependence was chosen as

$$\frac{d\sigma}{dp_T^2} \sim e^{-2p_T^2} \quad , \tag{10}$$

while we have used the similarity of the shape of the ρ^0 meson and f meson cross section [21] for the longitudinal dependence. To take account of the different resonance masses we assume

$$\frac{d\sigma}{dz} \simeq f(z) \quad , \tag{11a}$$

$$z = \frac{y}{y_{MAX}(m)} \quad , \tag{11b}$$

where $y_{MAX}(m)$ is the maximal kinematically allowed rapidity for particles with mass m at a given value of p_T and we assume that f(z) does not depend explicitly on m. f(z) was fitted to the ρ^0 meson measurement [20]. The results of the analysis are collected in table 3.

4.2.4 g^0 meson production

Nearly no measurements of g^0 meson production in pp collisions exist up to now [22]. We have therefore chosen the rapidity parametrization of eq. (11) for the g^0 meson production. The p_T dependence has been derived from the well-known fit [23] of the transverse momentum spectra

$$\frac{d\sigma}{dp_T^2} \sim e^{-6E_T} \tag{12a}$$

$$e_T = \sqrt{p_T^2 + m^2} \quad , \tag{12b}$$

which corresponds for g^0 mesons to the expression

$$\frac{d\sigma}{dp_T^2} \sim e^{-1.5\ p_T^2} \quad . \tag{13}$$

The results from the cross section calculation are given in table 3. Our results are compatible with the recently published cross section at lower energies [22].

4.2.5 $\overline{K^{*0}}(892)$ meson production

Measurements at FNAL energies show [24] that the production cross section for the $K^{*0}(892)$ meson has a similar longitudinal and transverse

behaviour as the K^- meson, if mass effects are taken into account. We have therefore fitted the function f(z) of formula (11) to the K^- meson cross section. The transverse momentum dependence of the cross section was parametrized by [25]

$$\frac{d\sigma}{dp_T^2} \sim e^{-3p_T^2} \tag{14}$$

The resulting cross sections are entered into table 3.

4.2.6 $\overline{K^{*0}}(1430)$ meson production

No differential distribution for the production of the $\overline{K^{*0}}(1430)$ meson in pp collisions exist up to now [24,26]. Therefore, we have used again the ansatz (11), fitted to K^- meson data, to parametrize the longitudinal dependence of the cross section. The p_T dependence was determined according to formulae (12)

$$\frac{d\sigma}{dp_T^2} \sim e^{-1.7\ p_T^2} \tag{15}$$

The cross sections for $\overline{K^{*0}}(1430)$ meson production are listed in table 3.

4.2.7 ϕ meson production

We have used the result from $\mu^+\mu^-$ pair production at $\sqrt{s}$ = 6.8 GeV [27]

$$x\,\frac{d\sigma}{dx} \sim (1-x)^4 \pm 0.4 \tag{16}$$

to describe the longitudinal behavour of ϕ meson production. A flatter x dependence was observed at ISR energies [28], but within its large error limits it is compatible with ansatz (16). Since different experiments have measured transverse momentum dependences fluctuating over a broad interval [29], we have used in the present analysis the parametrization

$$\frac{d\sigma}{dp_T^2} \sim e^{-2.5\ p_T^2}\ , \tag{17}$$

which is compatible with formula (12). The results of our analysis are given in table 3.

5. DISCUSSION OF THE RESULTS

5.1 Comparison with the results of other experiments

At high energies the data on vector and tensor meson production are scarce, nearly no measurements of differential cross sections in a given phase space region exist. We therefore compare the total cross sections, as determined in our experiment, with those of others at different energies. This procedure has the disadvantage that as an additional source of uncertainty the assumptions on the longitudinal and transverse momentum dependence of the production cross section enter.

In fig. 6 the total production cross section of ρ^0 mesons in various hadronic interactions is given [30]. The result of the present experiment is in good agreement with those of other experiments. As expected for a central production mechanism [31,32(a)] the cross section rises with $\sigma \sim \ell n^2 s$ (solid line). The comparison of the $p\bar{p} \to \rho^0 + x$ and the $pp \to \rho^0 + x$ cross sections at low and high energies supports this interpretation [31,32(a)].

The energy dependence of the f meson production cross section for different hadronic interactions is given in fig. 7 [32]. Again the result of our experiment is in good agreement with the extrapolated result of experiments at lower energies (solid line). The discrepancy with the other ISR measurement [26] is partially due to the different parametrization chosen for the longitudinal and transversal dependence of the production cross section. In addition, ref. [26] only considers statistical errors, therefore the error bars of that experiment have to be increased, if one wants to compare its results with the present one on equal footing. In agreement with the conclusions of ref. [31] the increase of the cross section with $\ell n^2 s$ and the different behaviour of $p\bar{p} \to f + x$ and $pp \to f + x$ reactions demonstrate that the central production mechanism dominates at high energies.

In the present experiment the g^0 meson production cross section was measured for the first time in pp collisions at ISR energies. It is about a factor three smaller than the f meson cross section at the same energy.

In fig. 8 the production cross section for K^0_s mesons is plotted as a function of $\sqrt{s}$ [33]. As for ρ^0 meson and f meson production the measurements at large energies are compatible with a dominant central production mechanism.

The total production cross section for the $\overline{K^{*0}}(892)$ meson is plotted as a function of c.m. energy in fig. 9 [34]. The result of our experiment is in good agreement with the extrapolated cross sections at lower energies. The observed s dependence and the vanishing difference between K^* and $\overline{K^*}$ meson production indicate again the dominance of a central production mechanism at high energies.

The observed $\overline{K^{*0}}(1430)$ meson cross section of (1 ± 0.25)mb (table 3) is in agreement with the expectation, which can be derived from the result of a FNAL experiment [24]

$$\frac{1}{2}\,\sigma(K^{*+}(1430) + \sigma(K^{*-}(1430)) = (1.6 \pm 0.85)\text{mb} .$$

The cross section of ref. [26] is appreciably smaller, it is based on a resonance signal of two-standard deviations.

The energy dependence of the ϕ meson production cross section is shown in fig. 10. The results of the different experiments [29] are in good agreement. Again the rise of the cross section indicates a dominating central production cross section.

5.2 Comparison of production cross sections for different mesons

In figs 11(a) and (b) the production cross section of ρ^0 and f mesons relative to π mesons are plotted as a function of energy. Within the errors these ratios are energy independent. It is interesting to note that the mean value

$$\frac{\sigma(pp \to \rho^0 + x)}{\sigma(pp \to \bar{\pi} + x)} = 0.13 \pm 0.01 \qquad (18a)$$

is the same as that observed in the current fragmentation of $\bar{\nu}p$ interactions [35]. A possible interpretation is that the fragmentation process of partons into mesons is universal and independent of the environment. Moreover, fig. 11(b) shows that also the ratio

$$\frac{\sigma(pp \to f + x)}{\sigma(pp \to \pi^- + x)} = 0.025 \to 0.005 \qquad (18b)$$

is energy independent.

The apparent suppression of the vector and tensor meson production as compared to the π^- meson production eq. (18a,b) can partly be explained by the observation that π^- meson are produced both directly and by resonance decay. This is demonstrated by fig. 12, where the ratios of eq. (18a,b) are plotted as a function of p_T. The ratios f/π^- and ρ^0/π^- increase steeply for small p_T, the phase space region populated by decay products of resonances. It is interesting to note that the ratios seem to level off at a value which differs from the statistical weight factor (2J+1). Such a deviation is also observed for the ratio $\sigma(f)/\sigma(\pi)$.

No simple explanation for this observation exists. Besides the suppression of angular momentum states $L \neq 0$ compared to $L = 0$ mesons [36], the strong mass dependence of the production cross sections shown in fig. 13 has to be considered. The production cross sections of mesons decrease exponentially with increasing particle masses. This behaviour is expected in thermodynamic quark parton models [37]. According to fig. 13 the production of resonances with strangeness is suppressed compared to non-strange resonances. This suppression is attributed to the SU(3) symmetry breaking of the quark sea [36]. The cross section for D^0 and D^+ meson production [10] fall on the same line as the strange particles, which may be taken as a hint that in hadronic interactions the strange and charm sea are suppressed by about the same amount [38].

To derive a quantitative measure of the suppression of strange particle production due to the SU(3) symmetry breaking of the quark sea, we have analyzed our results in the framework of the additive quark parton model of Shekhter et al., [36]. In their analysis particle productions in the central and fragmentation region was allowed for. We have determined the relative contribution of these two mechanisms of particle production at $\sqrt{s}$ = 52 GeV from measured $\pi^\pm$, $K^\pm$ inclusive cross sections.
To minimize the disturbing resonance decay we determined the suppression factor $\lambda = (0.30 \pm 0.10)$ of strange particle production from the ratio $\sigma(\overline{K^{*0}(1430)})/\sigma(f)$. This result is in good agreement with the value

derived by Shekhter et al., [36] using measurements at low energies. It is interesting to note that a recent analysis of the SU(3) symmetry breaking of the quark sea in ν interactions [39] derives a similar value for λ.

Using the vector and tensor meson cross sections as observed in the present experiment and taking into account isospin multiplets via Clebsch-Gordan coefficients we find that $\sim$ 55% of the π^- mesons are produced indirectly via the vector and tensor mesons observed in our investigation. Details of this calculation are given in ref. [5].

The ϕ meson production fits nicely into a phenomenological scaling behaviour [40], which correlates the production of ϕ, ψ and T mesons. A plot, using the most recent decay width of these resonances [14,41] is shown in fig. 14. Though the measured cross sections of these resonances differ by orders of magnitude, in the scaling plot the cross sections show a universal dependence on $1/\tau = S/M^2$. The full line in fig. 14 is a fit to the data, resulting in a

$$\frac{M^3}{\Gamma}\,\sigma \sim \frac{1}{\sqrt{\tau}}\,(1 - \sqrt{\tau})^{10} \text{ dependence .}$$

6. CONCLUSION

We have studied the production of the vector and tensor mesons ρ^0, f, g^0, $\overline{K^{*0}}(892)$, ϕ and $\overline{K^{*0}}(1430)$ at $\sqrt{s}$ = 52.5 GeV. Extrapolating the measured differential cross sections from the experimentally accessible phase space region ($\langle y \rangle$) = 2.6, $\langle p_T \rangle$ = 1.1 GeV/c) to the full phase space, we arrive at the following conclusions:

(i) The measured cross sections agree with the extrapolated values from experiments at lower energies. The observed rise with energy is compatible with a central production mechanism.

(ii) For the ϕ meson production cross section a phenomenological scaling law is fulfilled, which holds for ϕ, ψ and T mesons.

(iii) A common dependence of the production of mesons with given strangeness is observed. Using the approximations of the additive quark model we derive a strangeness suppression factor $\lambda = (0.30 \pm 0.10)$.

(iv) From the measured resonance cross section of the present experiment and isospin arguments (to allow for different charge states) we estimate that > 55% of all π^- and K^- mesons are decay products of resonances.

Acknowledgements

This experiment was greatly helped by contributions from the SFM detector group. We are indebted to H.F. Hoffmann and the ISR Experimental Support Group. We are grateful to Dr. J. Moritz (Karlsruhe) for his important contribution to design, and construction of the Cerenkov counters, and to K. Ratz for his technical help. The Dortmund and Heidelberg groups were supported by a grant from the Bundesministerium für Forschung und Technologie of the Federal Republic of Germany, the Collège de France group was funded by IN2P3 and the CEA. The experiment has been supported in part at an earlier stage by the Kernforschungszentrum Karlsruhe.

REFERENCES

[1] D.R.O. Morrison, Proceedings of the VIIth International Colloquium on Multiparticle Reactrions, Tutzing 1976, p. 73

[2] CCHK Collaboration, D. Drijard et al., Nucl. Phys. B155 (1979) 269 (and references quoted therein)

[3] W. Kittel, Hadron-hadron Interactions at low p_T and Partons, Proceedings of the Xth Symposium on Multiparticle Dynamics, Goa 1979, p. 1

[4] W. Ochs, Nucl. Phys. B118 (1977) 397

K.P. Das and R.C. Hwa, Phys. Lett. 68B (1977) 459

F.C. Erne and J.C. Sens, CERN Preprint 1978 and ref. [18]

[5] J. Spengler, Ph.D. Thesis, University of Dortmund 1980 (unpublished)

[6] CCHK Collaboration, M. Della Negra et al., Nucl. Phys. B127 (1977) 1

CCHK Collaboration, D. Drijard et al., Nucl. Phys. B156 (1979) 309

[7] W. Bell et al., Nucl. Instr. & Meth. 125 (1975) 437

[8] CCHK Collaboration, M. Della Negra et al., Phys. Lett. 59B (1975) 481

P. Hanke, Ph.D. Thesis, University of Karlsruhe 1976 and KfK Report 2412 (1977)

[9] P. Capiluppi et al., Nucl. Phys. B79 (1974) 189

[10] ACCDHW Collaboration, D. Drijard et al., Phys. Lett. 81B (1979) 250 and preliminary results quoted in W. Geist, contribution to the Topical workshop on Forward Production of High Mass Flavours at Collider Energies, Paris, November 1979, Ed. G. Fontaine L.P.C.80.13

[11] ACCDHW Collaboration, D. Drijard et al., Phys. Lett. 85B (1979) 452

[12] P.H. Higgins et al., Phys. Rev. D19 (1979) 65

[13] J.D. Jackson, Nuovo Cimento 34 (1964) 1644

[14] Particle Data Group, Rev. Mod. Phys. 52 (1980) No. 2

[15] J.J.J. Kokkedee, The Quark Model, W.A. Benjamin, New York 1969

[16] V. Blobel et al., Phys. Lett. 48B (1974) 73

[17] B. Alper et al., Nucl. Phys. B87 (1975) 19

B. Alper et al., Nucl. Phys. B100 (1975) 237

M. Antinucci et al., Lett. al Nuovo Cimento 6 (1973) 121

B. Alper et al., Phys. Lett. 47B (1973) 75

A.M. Rossi et al., Nucl. Phys. B84 (1975) 269

REFERENCES (Cont'd)

[18] J. Singh et al., Nucl. Phys. B140 (1978) 189

[19] H. Kichimi et al., Phys. Rev. D20 (1979) 37

[20] M.G. Albrow et al., Nucl. Phys. B155 (1979) 39

[21] A. Suzuki et al., Lett. al Nuovo Cimento 24 (1979) 449

[22] A. Suzuki et al., Nucl. Phys. B172 (1980) 327

[23] H. Satz, Phys. Rev. D17 (1978) 914

[24] H. Kichimi et al., Lett. al Nuovo Cimento 24 (1977) 129

[25] K. Böckmann et al., CERN/EP 79-131

[26] A. Böhm et al., Phys. Rev. Lett. 41 (1978) 1761

[27] K.J. Andersson et al., Phys. Rev. Lett. 37 (1976) 799

[28] M.M. Block et al., CERN/EP 79-82

[29] D.R.O. Morrison, CERN/EP 79-102, and references quoted in this paper

[30] Proton-proton interactions (refs [16,20,21,26]):

(a) R. Singer et al., Phys. Lett. 60B (1976) 385
(b) V.V. Ammosov et al., Sov. J. Nucl. Phys. 24 (1976) 30
(c) H. Nussbaumer, Diplomarbeit, Bonn 1977 $\bar{p}p$ interactions;
(d) D. Gall et al., Proc. Int. Symp. $\bar{p}p$ interactions, Loma-Koli, Finland 1975
(e) R. Raja et al., Phys. Rev. D16 (1977) 2733
(f) P.S. Gregory et al., Nucl. Phys. B119 (1977) 60
(g) R. Hamatsu et al., Nucl. Phys. B123 (1977) 189
(h) D.I. Ermilova et al., Nucl. Phys. B137 (1978) 29
(i) M. Markytan et al., Nucl. Phys. B143 (1978) 263
(j) Y.I. Arestov et al., IHEP 79-22
(k) V. Karimäki et al., HU-P-174 (1979) University of Helsinki, Finland

[31] K. Böckmann, Bonn-HE-77-24

[32] Proton-proton collisions (refs [25,21]): K. von Hold, Ph.D. Bonn IR-79-24

Proton-antiproton collisions (refs [29e,29g,29i, 29k])

[33] Proton-proton collisions, ref. [19]:

(a) J. Whitmore, Phys. Rep. 10 (1974) 274
(b) J. Whitmore, Phys. Rep. 27 (1976) 188
(c) F.T. Dao et al., Phys. Rev. Lett. 30 (1973) 1151
(d) H. Boggild et al., Nucl. Phys. B57 (1973) 77
(e) J.W. Chapmann et al., Phys. Lett. 47B (1973) 465

REFERENCES (Cont'd)

(f) H. Blumenfeld et al., Phys. Lett. 45B (1973) 528
(g) A. Sheng et al., Phys. Rev. D11 (1975) 1733
(h) K. Jaeger et al., Phys. Rev. D11 (1975) 1756 and 2405
(i) R. Singer et al., Nucl. Phys. B135 (1978) 265
(j) M. Alston-Garnjost, Phys. Rev. Lett. 35 (1975) 142
(k) R.D. Kass et al., Phys. Rev. D20 (1979) 605
(l) H. Brink et al., Nucl. Phys. B164 (1980) 1
(m) J. Hofmann, Ph.D. Thesis, Bonn-IR-77-34 ($\bar{p}p$ collisions ref. [32a,b]
(n) F.T. Dao et al., Phys. Lett. 51B (1974) 505
(o) M.T. Regan et al., Nucl. Phys. B141 (1978) 65
(p) A.M. Cooper et al., Nucl. Phys. B136 (1978) 365

[34] See refs [16,23,24,29b,32i]

[35] M. Derrick et al., Phys. Lett. 91B (1980) 307

[36] V.M. Shekhter, L.M. Shcheglova, Sov. J. Nucl. Phys. 27 (1978) 567

[37] H. Bohr and H.B. Nielsen, Nucl. Phys. B128 (1977) 275

[38] S.J. Brodsky et al., Phys. Lett. 93B (1980) 451

[39] N. Schmitz, Proc. of the 1979 International Symposium on Lepton and Photon Interactions at High Energies, Fermilab 1979, p. 359

[40] F. Gaisser, M. Halzen and E.A. Paschos, Phys. Rev. D15 (1977) 2572

[41] H. Albrecht et al., Phys. Lett. 93B (1980) 500

TABLE CAPTIONS

Table 1 Resonances observed in the $\pi^-\pi^+$ meson channel
$N_{a,b,c}$ = number of events in the resonance channel as observed in figs 1(a-c) respectively.

Table 2 Resonances observed in the $K^-\pi^+$ and K^-K^+ meson channel.

Table 3 Cross section for resonance production as determined in the present experiment.

TABLE 1

	K^o_s	ρ^0	f^0	g^0
Na	640 ± 101	6189 ± 311	3824 ± 240	1257 ± 190
N_b/N_c	-	1.93 ± 0.16	0.18 ± 0.03	-
$N_a/(N_b + N_c)$	-	0.92 ± 0.05	1.04 ± 0.09	-

TABLE 2

	$\overline{K^{*0}}(892)$	$\overline{K^{*0}}(1430$	ϕ
N_a	2532 ± 204	1332 ± 171	108 ± 22
N_b/N_c	3.15 ± 0.38	0.48 ± 0.13	-
$N_a/(N_b + N_c)$	0.82 ± 0.07	0.95 ± 0.16	-

TABLE 3

	$\frac{d\sigma}{dy}\|_{y=2.6}$ (mb)	$\frac{d\sigma}{dp_T^2}\|_{p_T=1}$ (mb/GeV^2)	σ_{tot} (mb)
K^o_s	1.6 ± 0.46	1.3 ± 0.3	11.5 ± 2.5
ρ^0	4.1 ± 0.9	2.9 ± 0.6	22.0 ± 5.0
f^0	0.54 ± 0.12	1.7 ± 0.4	5.4 ± 1.2
g^0	0.25 ± 0.07	1.0 ± 0.27	2.2 ± 0.6
$\overline{K^{*0}}(892)$	0.25 ± 0.06	0.64 ± 0.15	4.3 ± 1.0
$\overline{K^{*0}}(1430)$	(38 ± 9)*10^{-3}	0.35 ± 0.08	1.0 ± 0.23
ϕ	0.13 ± 0.04	(9 ± 3)*10^{-3}	1.3 ± 0.35

FIGURE CAPTIONS

Fig. 1 Invariant mass spectrum of $\pi^-\pi^+$ meson system:

(a) all events;
(b) π^- and π^+ meson in same and
(c) in opposite azimuthal angular region.

The full line describes the non-resonant background as determined by event mixing.

Fig. 2 (a-c) Mass distribution from fig. 1 but after background subtraction.

Fig. 3 Same as fig. 1(a) for $K^-\pi^+$ meson system.

Fig. 4 Same as fig. 2(a) for $K^-\pi^+$ meson system.

Fig. 5 (a) same as fig. 1(a) K^-K^+ meson system; (b) same as fig. 2(a) for K^-K^+ meson system. The full line describes the 2σ background fluctuation.

Fig. 6 Total production cross section for ρ^0 mesons in hadronic interaction as a function of $\sqrt{s}$; ref. [29] and this experiment (●).

Fig. 7 Total production cross section for f mesons in hadronic interactions as a function of $\sqrt{s}$; ref. [31] and this experiment (●).

Fig. 8 Total production cross section for K^0_s mesons in hadronic interactions as a function of $\sqrt{s}$; ref. [32] and this experiment (●).

Fig. 9 Total production cross section for $K^*(892)$ in pp interactions as a function of $\sqrt{s}$; ref. [33] and this experiment (●).

Fig. 10 Total production of cross section of ϕ mesons in pp interactions as a function of $\sqrt{s}$; ref. [28] and this experiment (●).

FIGURE CAPTIONS (Cont'd)

Fig. 11 Comparison of ρ^0, f and π^- production as a function of $\sqrt{s}$. The cross (x) is the prediction of the additive quark parton model [35].

Fig. 12 Ratio of ρ^0/π^- (black points) and f/π^- (o) production cross sections as a function of p_T . (x), this experiment and ref. [66].

Fig. 13 Total production cross section at $\sqrt{s}$ = 52.5 GeV for mesons as a function of the resonance mass M.

Fig. 14 Comparison of ϕ, ψ' and Y meson production cross section as proposed by Gaisser et al., [39].

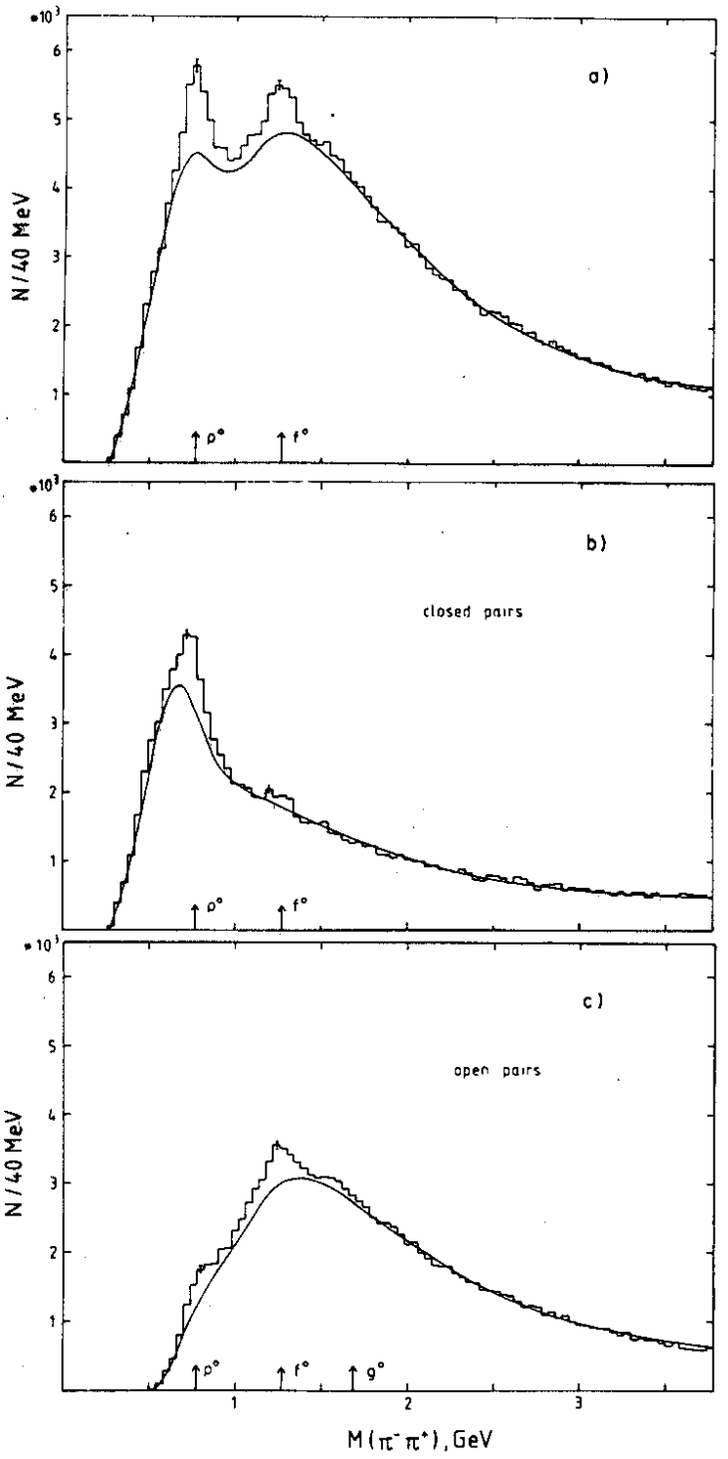

Fig. 1

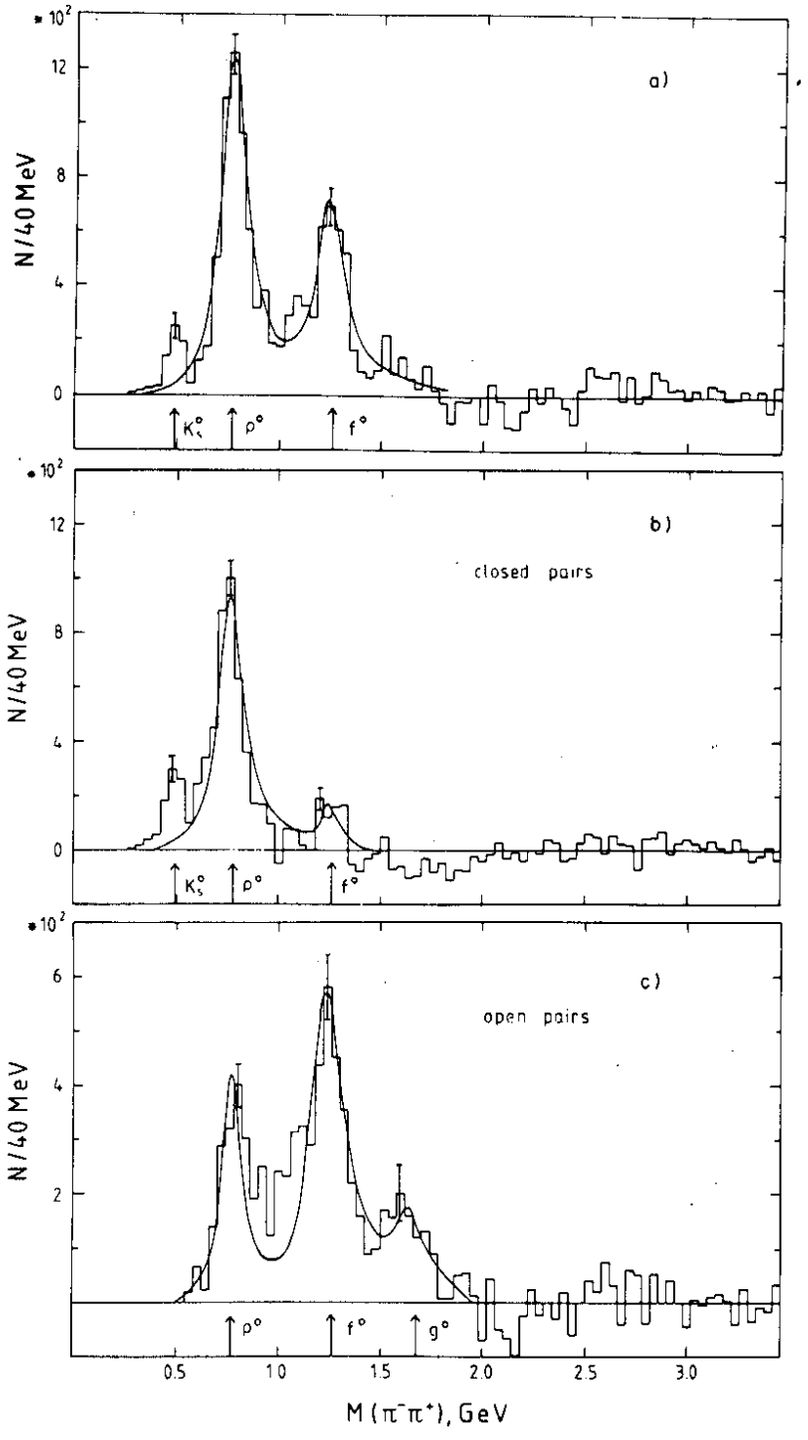

Fig. 2

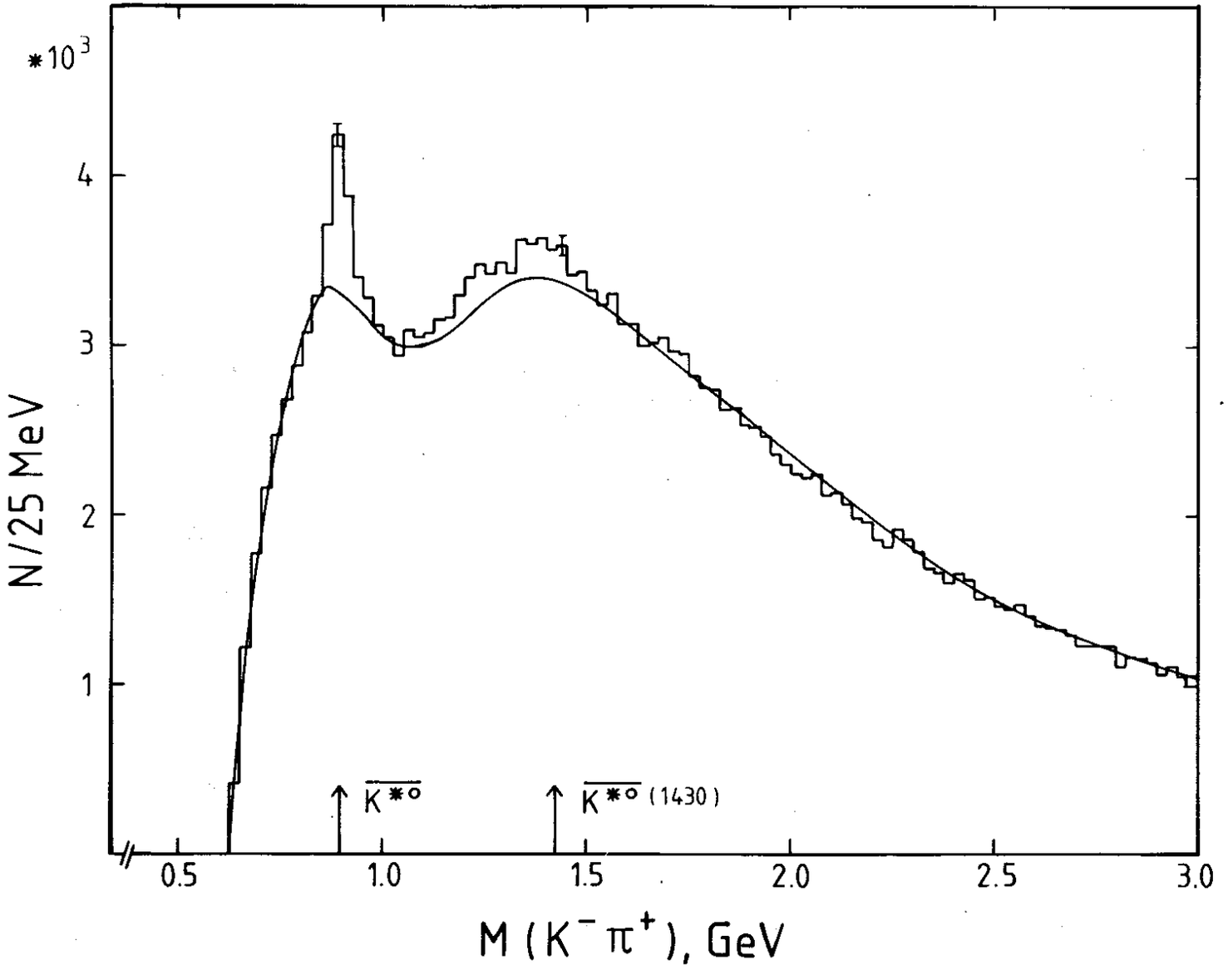

Fig. 3

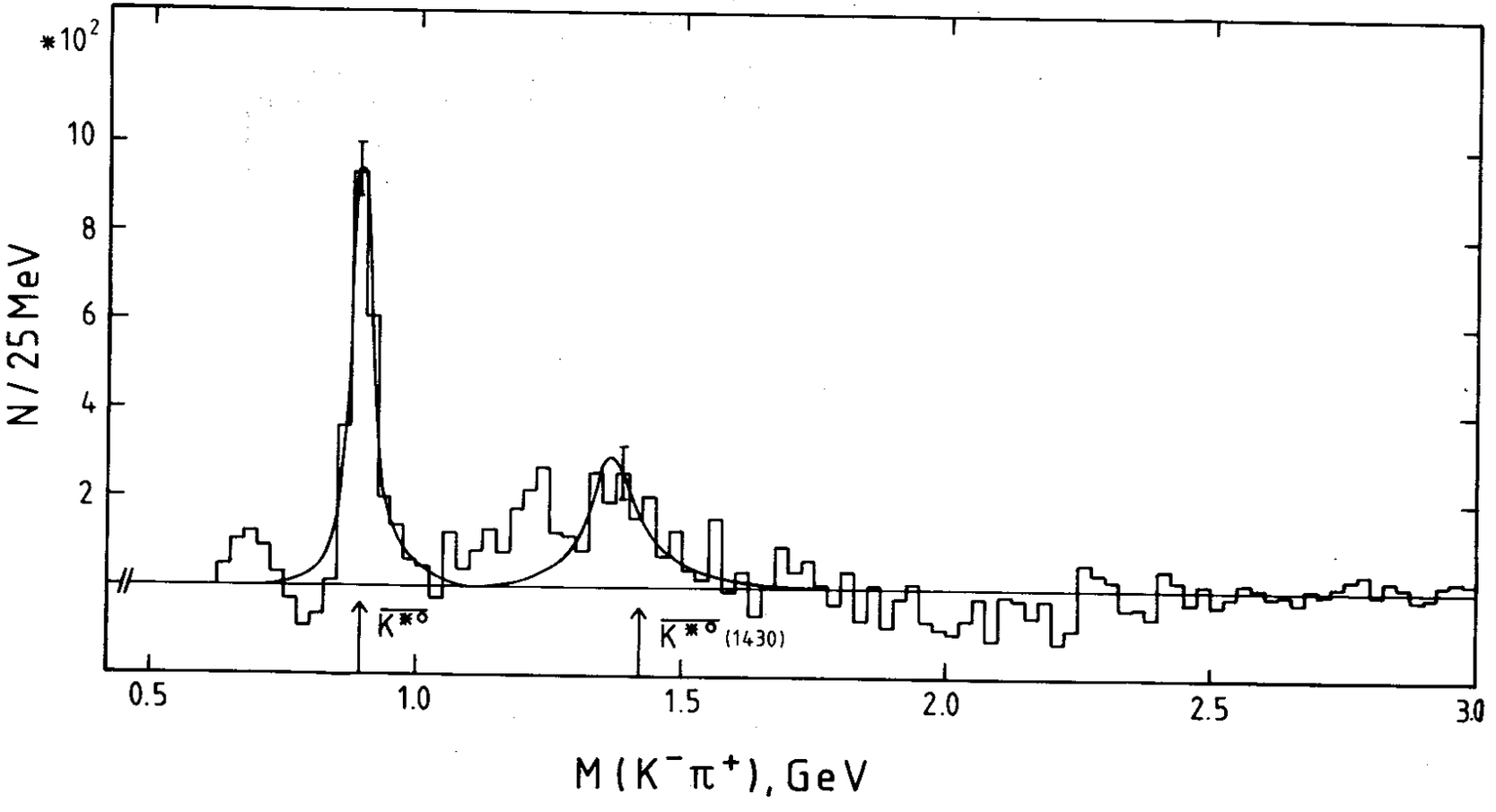

Fig. 4

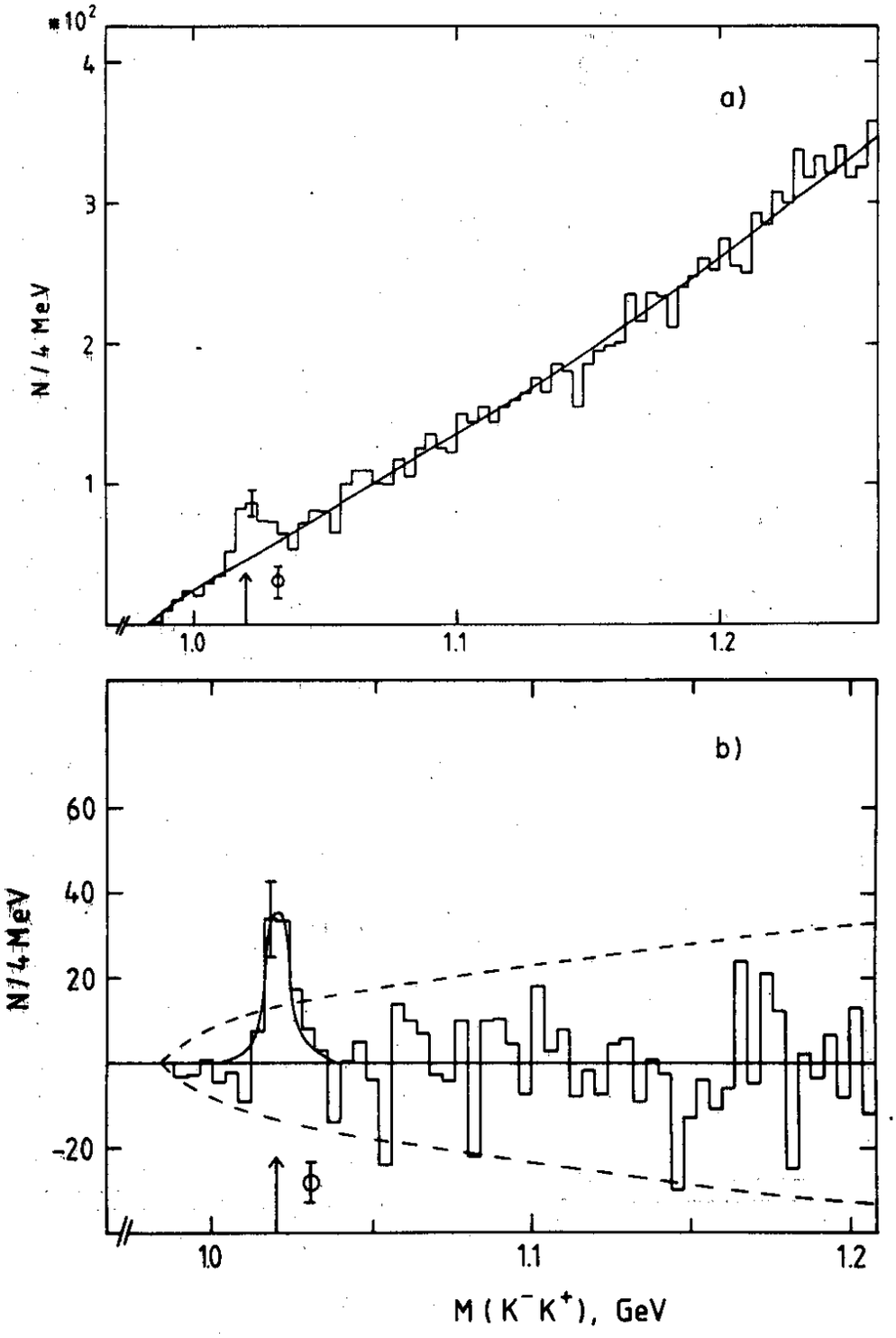

Fig.5

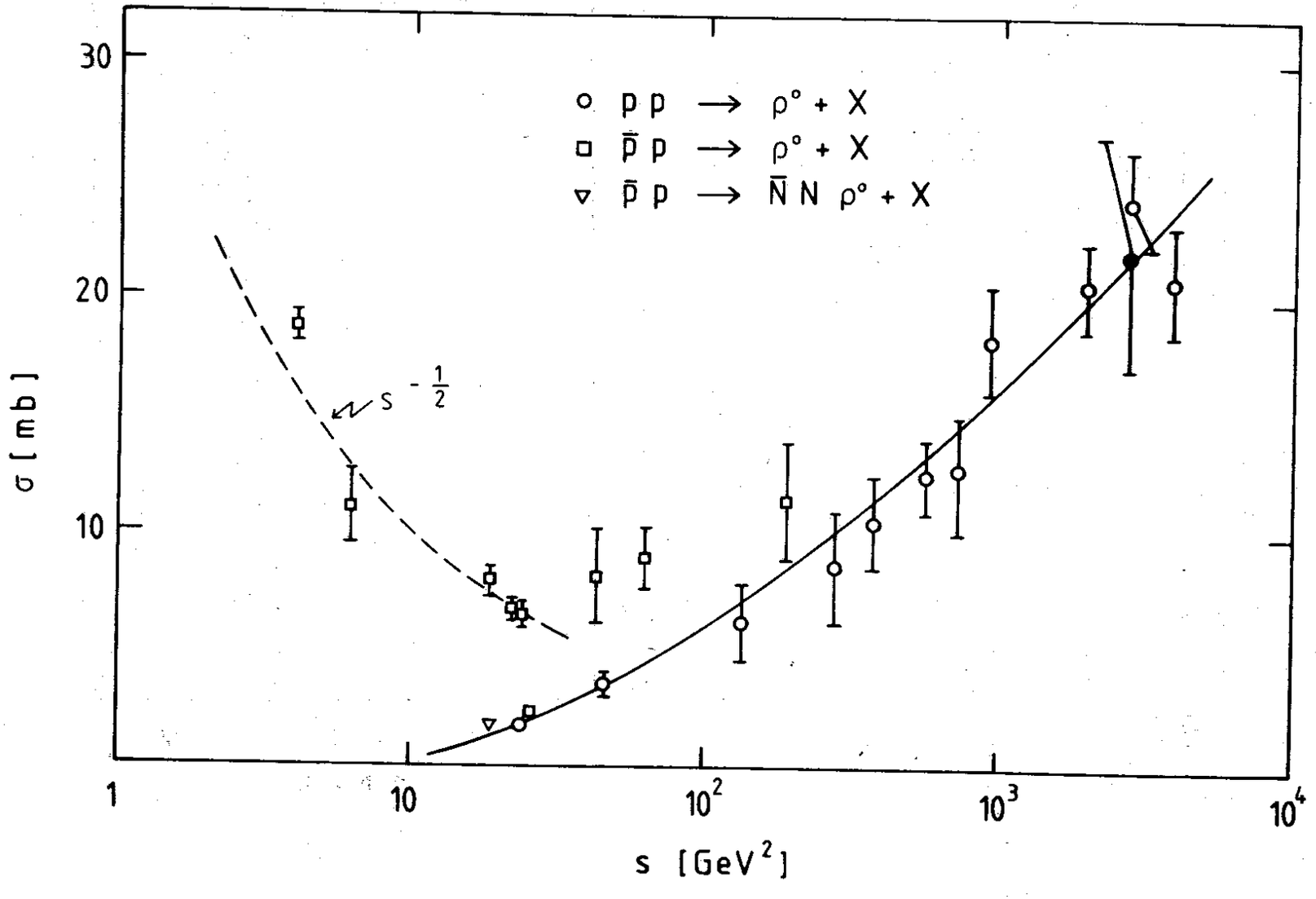

Fig. 6

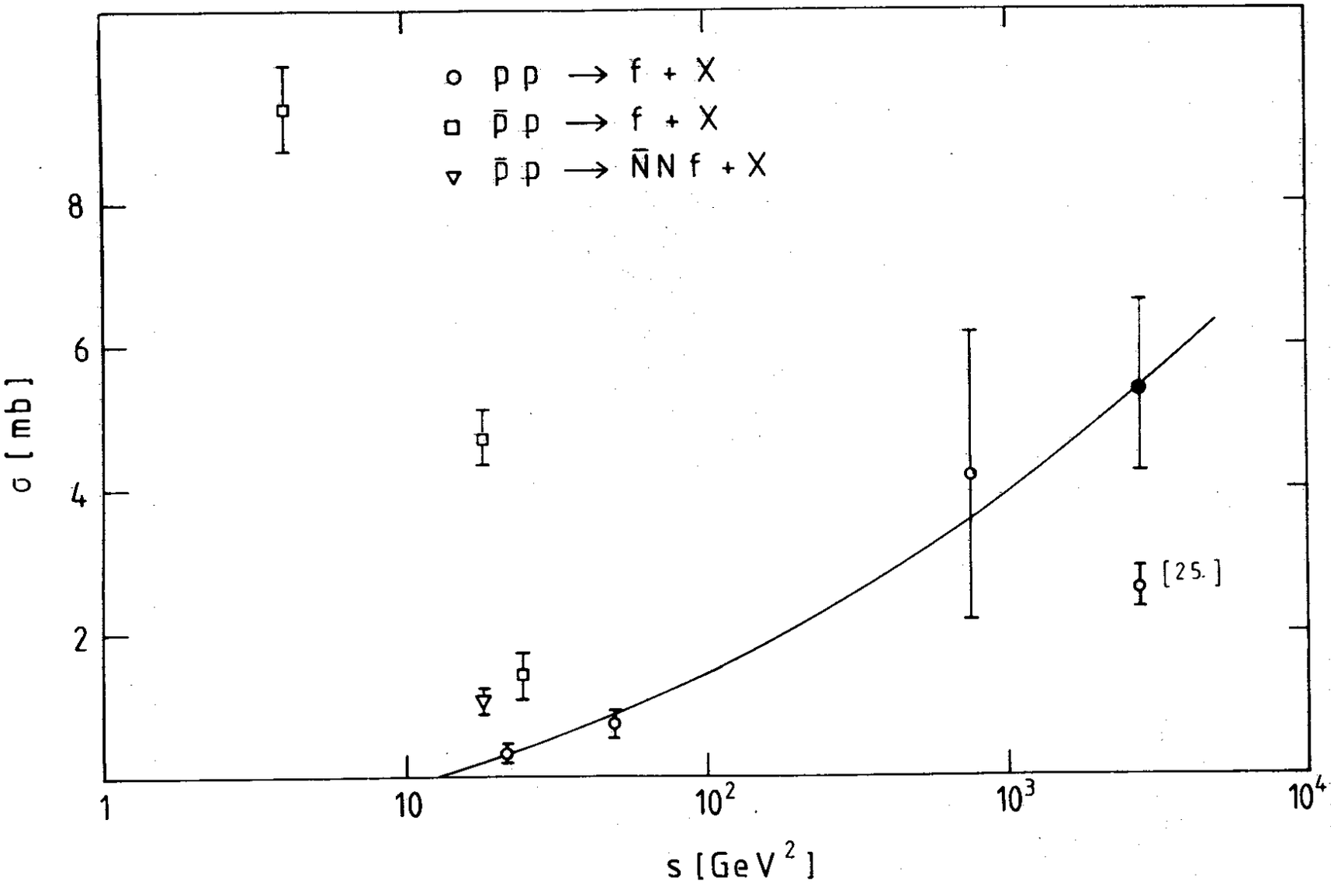

Fig. 7

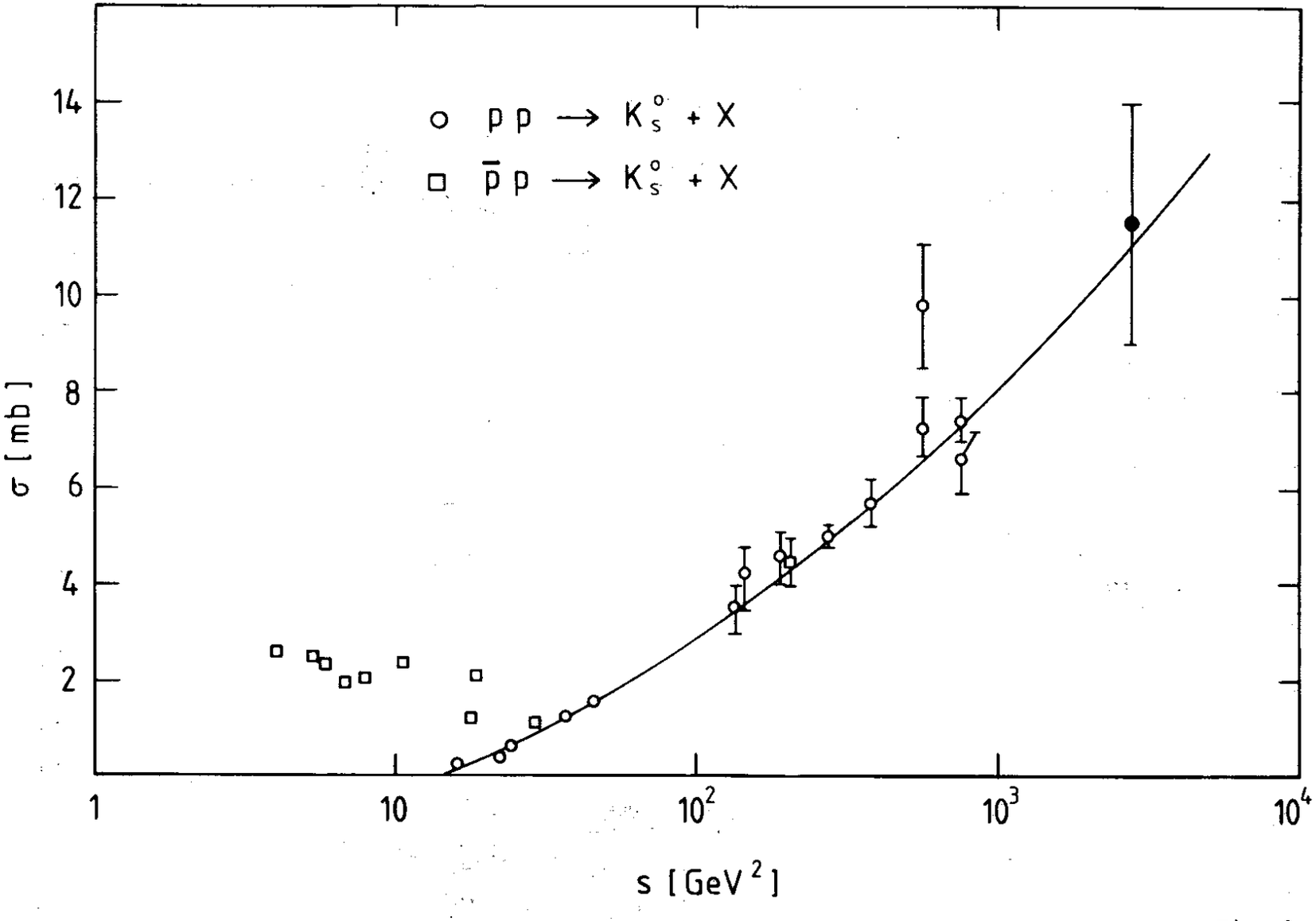

Fig. 8

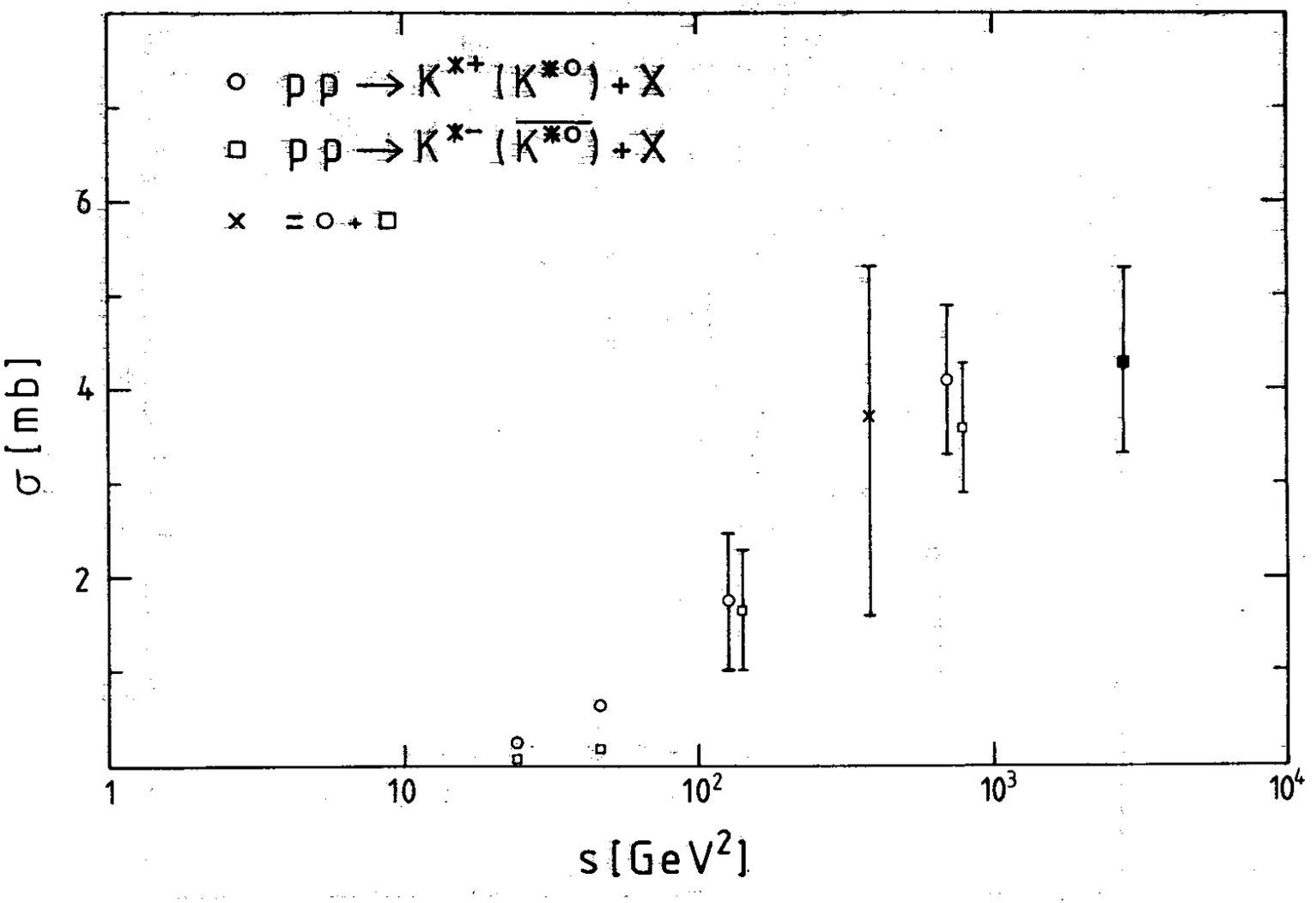

Fig. 9

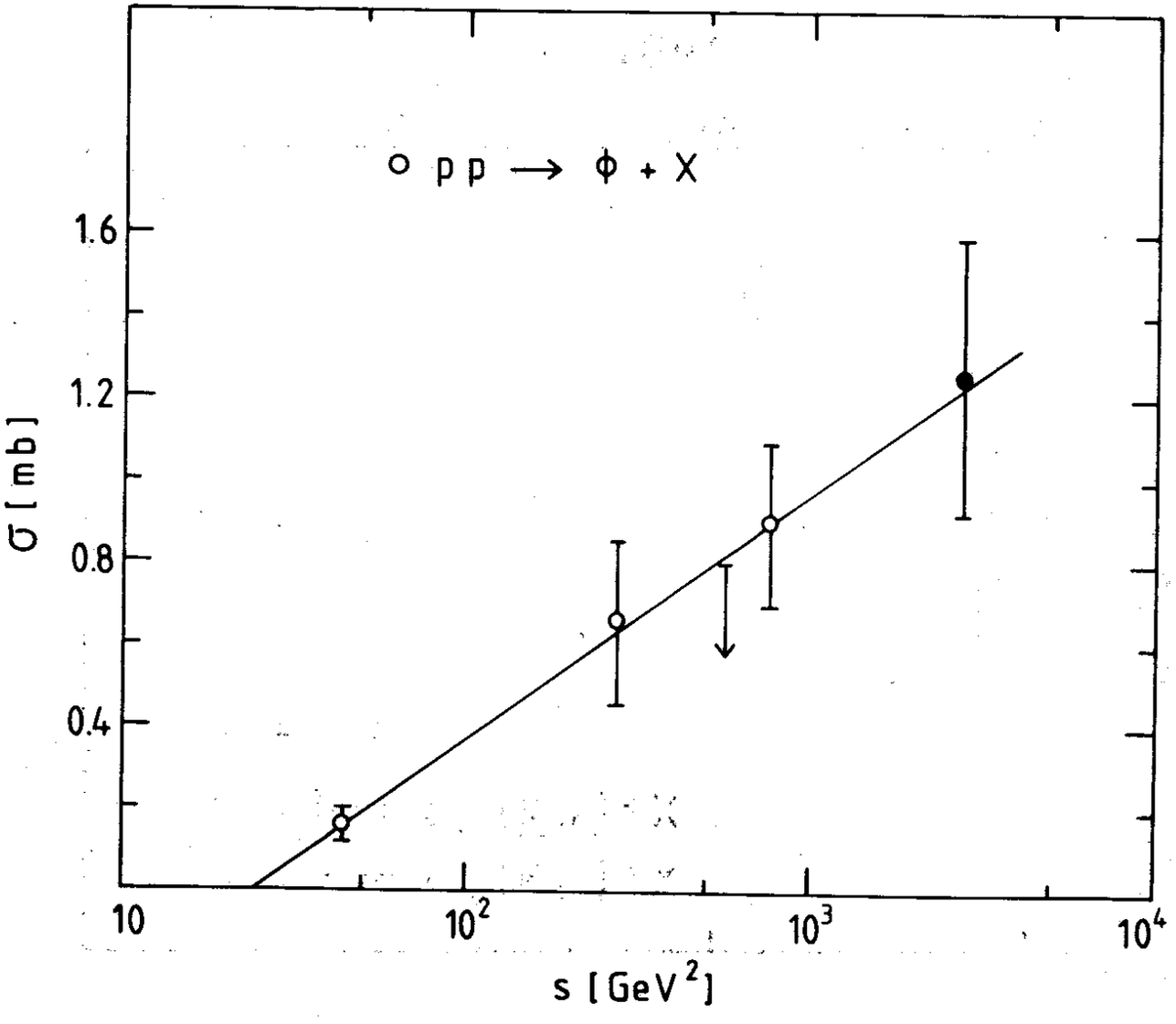

Fig. 10

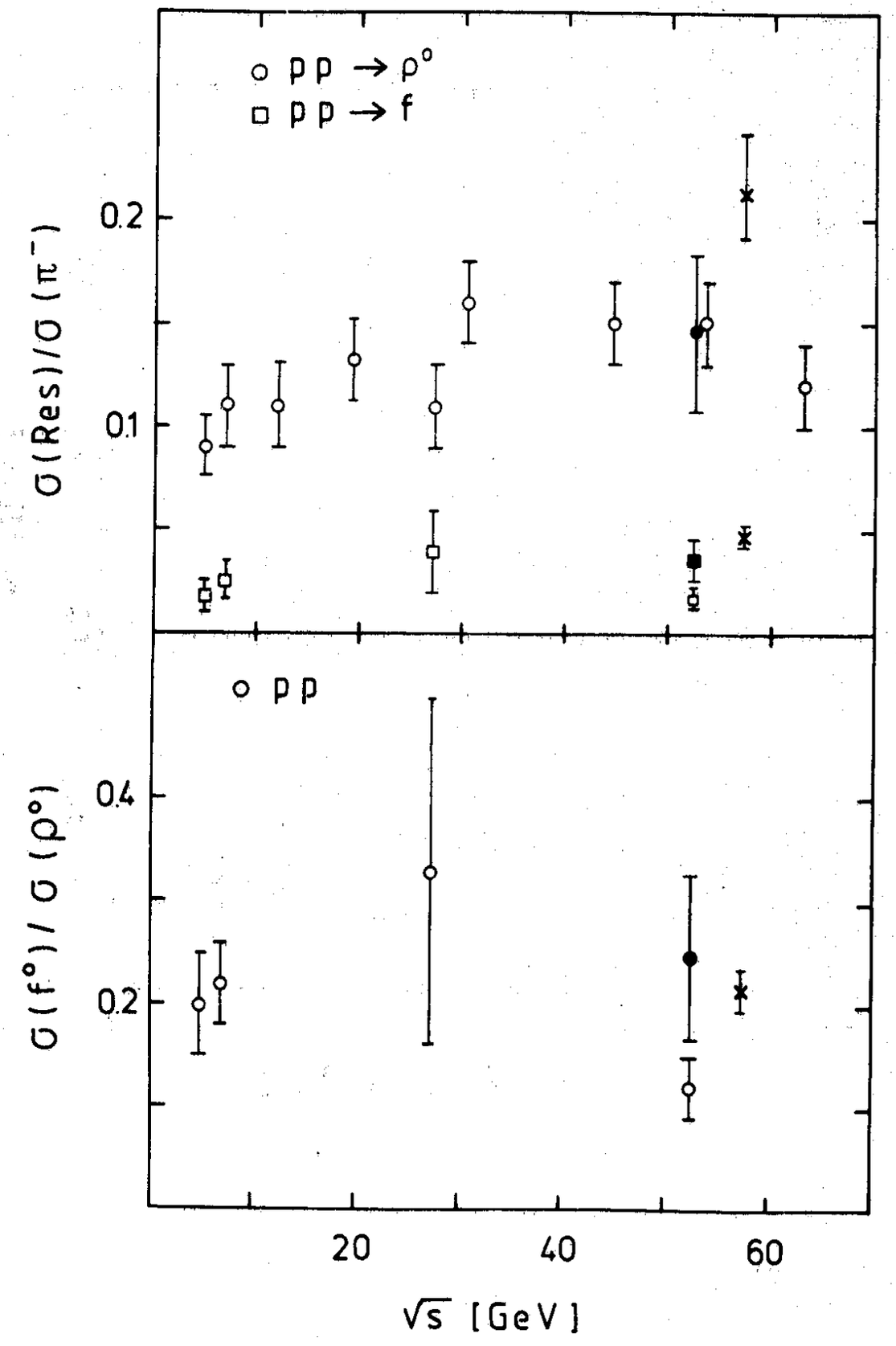

Fig. 11

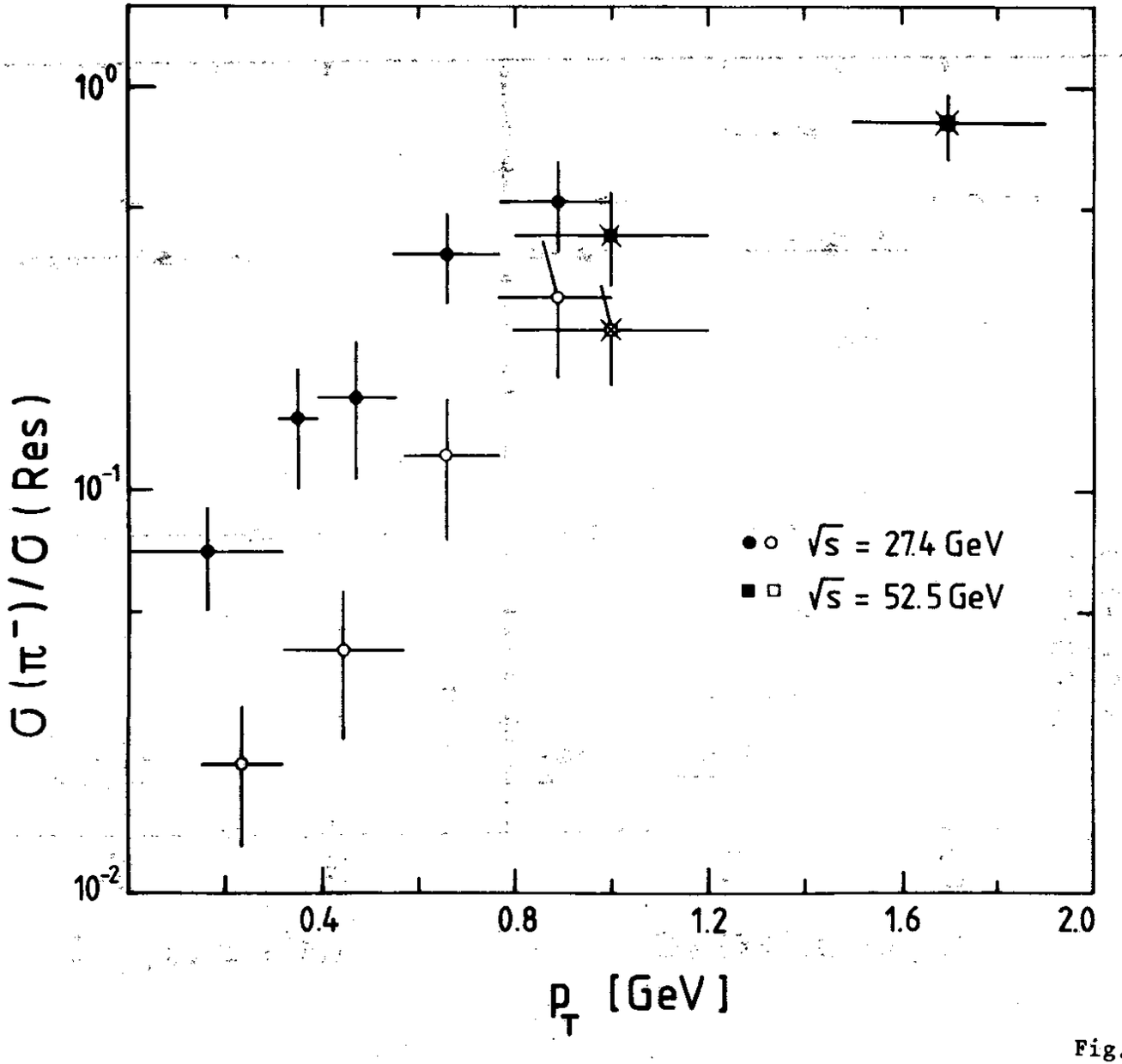
10^0
10^{-1}
10^{-2}
$\sigma(\pi^-)/\sigma(Res)$
0.4
0.8
1.2
1.6
2.0
p_T [GeV]
$\sqrt{s}$ = 27.4 GeV
$\sqrt{s}$ = 52.5 GeV

Fig. 12

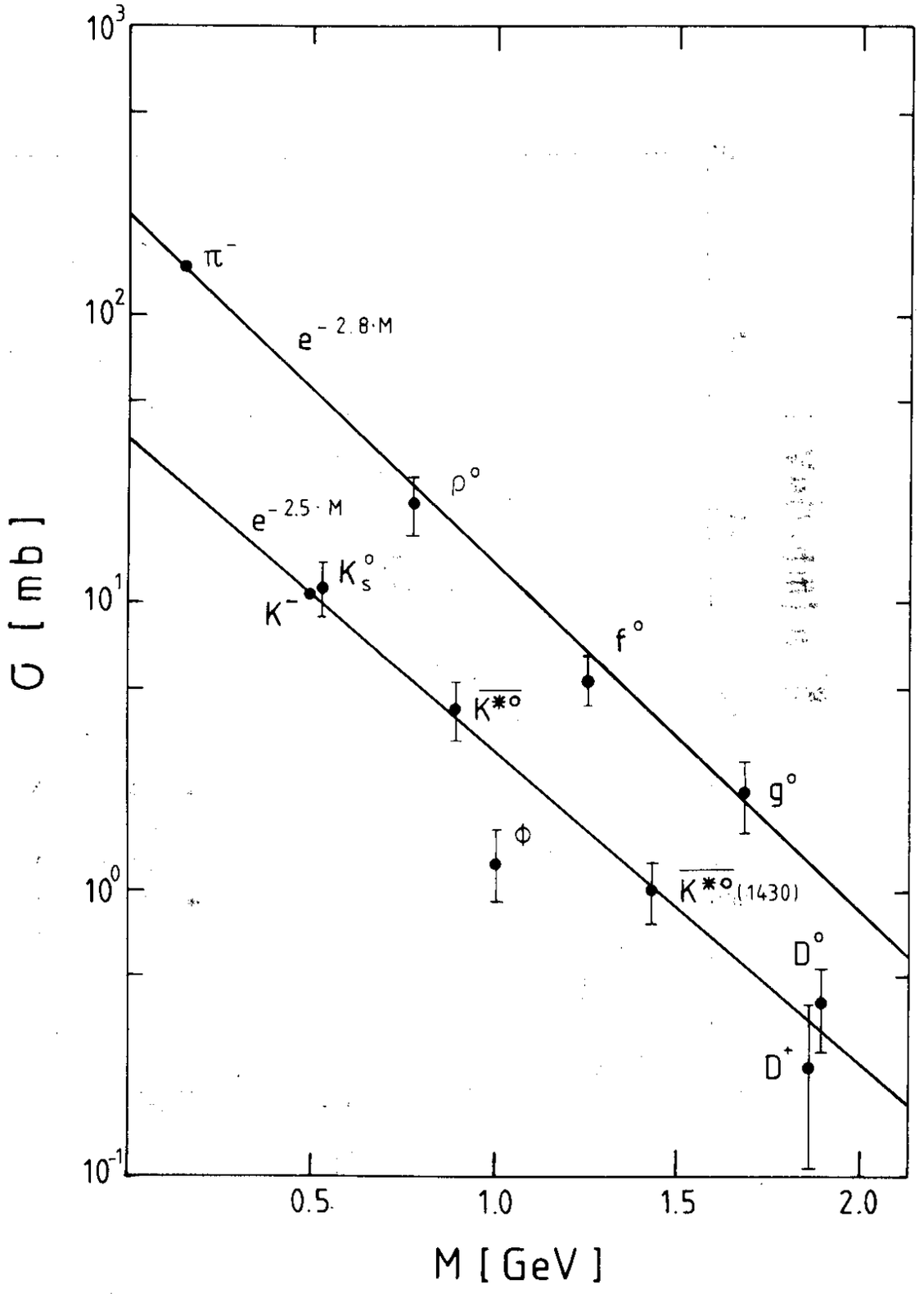
10^3
10^2
10^1
10^0
10^{-1}
σ [mb]
π^-
$e^{-2.8 \cdot M}$
$e^{-2.5 \cdot M}$
ρ°
K_s°
K^-
f°
$\overline{K^{*\circ}}$
g°
Φ
$\overline{K^{*\circ}}(1430)$
D°
D^+
0.5
1.0
1.5
2.0
M [GeV]

Fig. 13

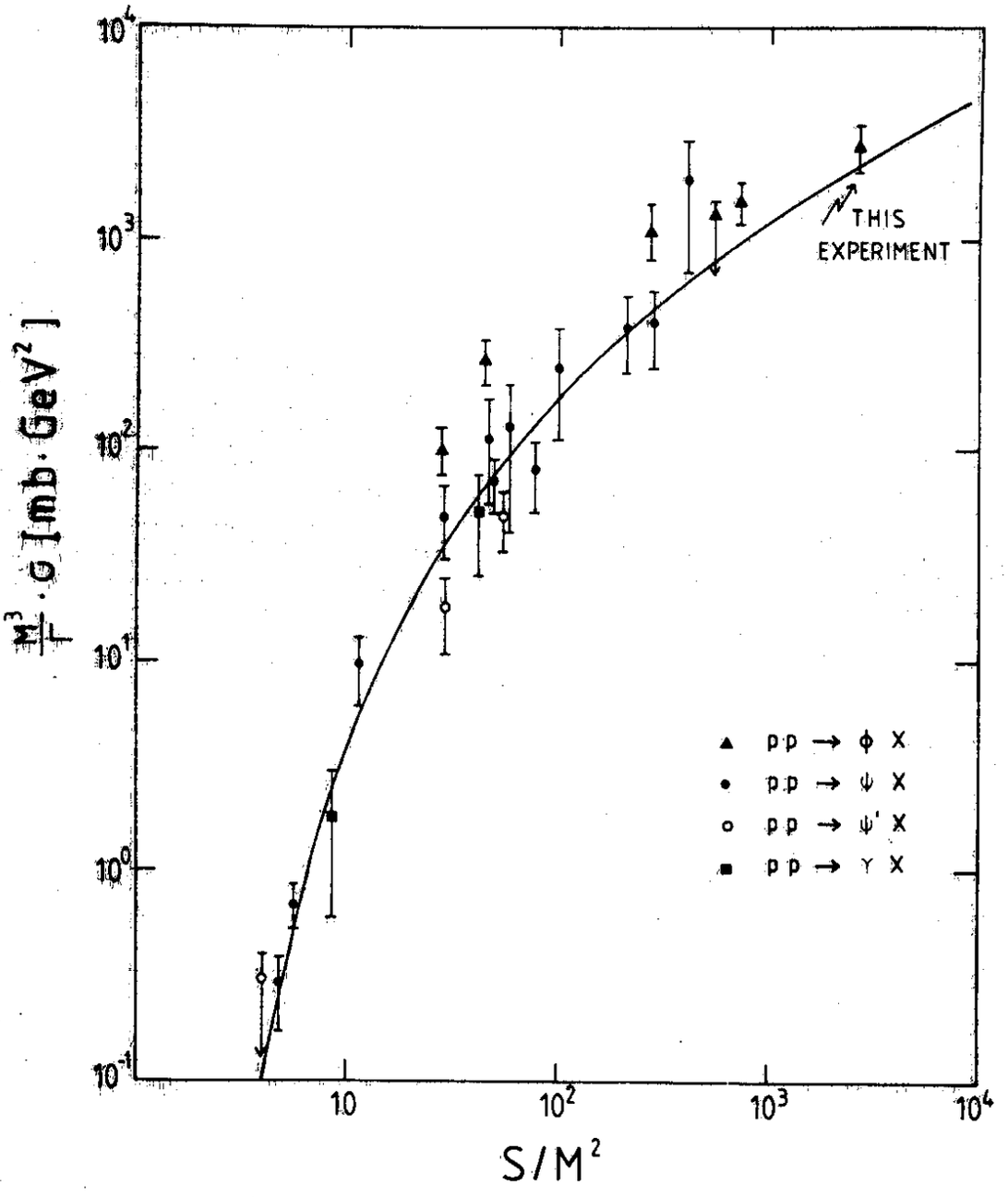
$\frac{M^3}{\Gamma} \cdot \sigma$ [mb · GeV^2]
10^4
10^3
10^2
10^1
10^0
10^{-1}
10
10^2
10^3
10^4
S/M^2
THIS EXPERIMENT
▲ p p → ϕ X
● p p → ψ X
○ p p → ψ' X
■ p p → ϒ X

Fig. 14